Thermal Analysis of Zone-Melting Recrystallization of Silicon-on-Insulator Structures with an Infrared Heat Source: An Overview

I. N. Miaoulis, P. Y. Wong, S. M. Yoon, R. D. Robinson, and C. K. Hess

Thermal Analysis of Materials Processing Laboratory, Department of Mechanical Engineering, Tufts University, Medford, Massachusetts 02155

ABSTRACT

Thermal processing of semiconductive multilayer thin film structures is used extensively for material quality enhancement. The quality of the resultant material is highly dependent on the heat transfer dynamics of the process. Although trial and error techniques are still used for process parameter optimization, efforts have been made to understand the fundamental heat transfer mechanisms involved. This paper presents an overview of studies on thermal issues that affect the material quality of multilayer thin film structures during processing with an infrared heat source. Emphasis is placed on investigations of zone-melting recrystallization of silicon-on-insulator structures using a graphite strip as a heat source. Studies on the conduction, macroscale and microscale radiation, processing chamber convection, scan speed, and constitutional supercooling are reviewed. Analyses of thermally driven instabilities at the solid-liquid interface are reported. Areas where further research is needed are also identified.

Thermal processing of multilayer thin film structures with an infrared heat source is commonly used during semiconductor wafer processing. A procedure that involves infrared heating by a moving line heat source is zone-melting recrystallization (ZMR) of silicon-on-insulator (SOI) wafers. The SOI structure offers several advantages over bulk silicon material for use in the electronics industry. Foremost, SOI wafers can be used in the fabrication of radiation-hardened electronics. Complementary metal oxide semiconductor (CMOS) circuits in SOI structures have a higher speed due to lower junction and metallization capacitances, smaller size, and elimination of latch-up, the last is a problem due to the presence of parasitic bipolar transistors in CMOS circuits. Also, field effect transistors (FET's) can be built over the insulator which is less sensitive to temperature changes than typical devices developed for bulk silicon. This allows circuit performance to be extended into higher temperature ranges.

ZMR processing of SOI films, using a graphite strip as a heat source, has been used over the past ten years to convert polycrystalline silicon films into single crystals for use in the fabrication of high-speed integrated circuits. This technology has recently produced successful memory chips.[1] Typical SOI film structures consist of a standard silicon crystal wafer (~525 μm thick) capped by successive thin films of silicon dioxide (~1 μm), polycrystalline silicon (~1 μm), and silicon dioxide (~1 μm) (Fig. 1). The film structure to be recrystallized is generally placed on a lower heater (susceptor) that raises the temperature of the wafer to a temperature just below the melting point of silicon. A graphite strip heats the top side of the wafer and establishes a narrow molten zone in the silicon film to be recrystallized (Fig. 2). The graphite strip is then slowly moved across the surface of the material. As the silicon film freezes behind the strip, a single crystal forms.

Previous studies have shown that crystal growth strongly depends on the control of the temperature profile within the silicon.[2,3] Depending on the width of the melt-zone, varying qualities of films are developed.[1] The most common imperfections found in structures processed by ZMR are low-angle sub-grain boundaries (sub-boundaries). Dislocation trails or clusters are also common. Sub-boundaries are defined as defects that exhibit a crystallographic angular misalignment on the order of 1° from the growth axis.[4] Various combinations of low scan speeds with low thermal gradients produced sub-boundary free SOI structures.[2]

Although trial and error techniques are still used for process parameter optimization, efforts have been made to understand the fundamental heat transfer mechanisms involved. The scope of this paper is to present an overview of the thermal issues during thermal processing of multilayer thin film structures with an infrared line heat source such as a graphite strip.The authors compiled information from recent literature focusing primarily on ZMR of SOI structures.

In typical ZMR processes the SOI structure is placed in a water-cooled vacuum chamber (Fig. 3) that surrounds the heating elements (bottom heater and graphite strip). The chamber is filled with an inert gas such as helium or argon. In some cases there is a continuous flow of the inert gas during processing. All three heat transfer modes (conduction, convection, and radiation) play roles of varying significance during ZMR processing. In addition, other related effects induced by the motion of the strip heater, constitutional supercooling, microscale phenomena, and the solid/liquid interface morphology, play critical roles during such a process. Each of these topics is presented separately.

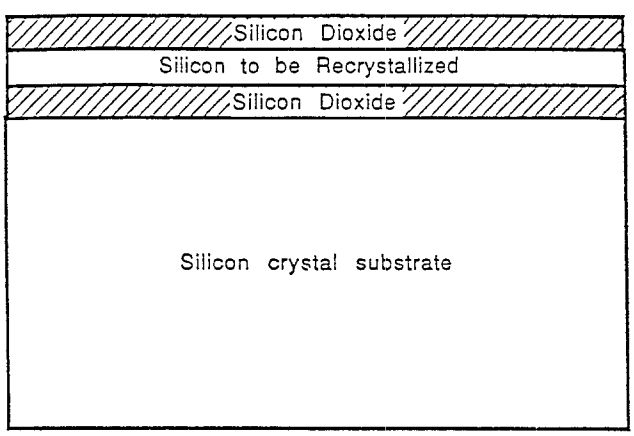

Fig. 1. Schematic of SOI film structure.

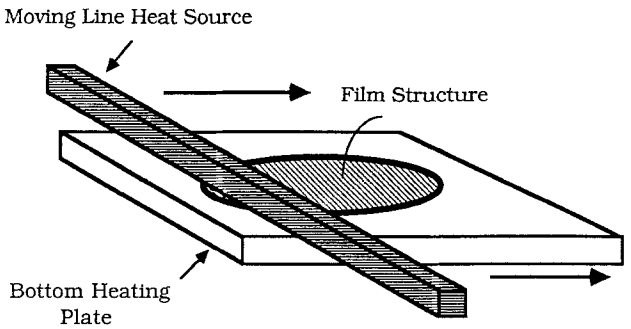

Fig. 2. Schematic of the ZMR process.

Heat Conduction

The three-dimensional heat conduction in the film structure can be expressed by the general expression

$$\rho c_p \frac{\partial T}{\partial t} = \frac{\partial}{\partial x}\left(k\frac{\partial T}{\partial x}\right) + \frac{\partial}{\partial y}\left(k\frac{\partial T}{\partial y}\right) + \frac{\partial}{\partial z}\left(k\frac{\partial T}{\partial z}\right) + S \qquad [1]$$

where ρ is the density, c_p is the specific heat, k is the thermal conductivity, T is the temperature, t is the time, and S is the rate of heat generation per unit volume. Since the temperature distribution is uniform in the direction of the axis of the strip heater, the heat conduction equation can be reduced to two dimensions. With the appropriate boundary conditions, the temperature profiles in the wafer can be obtained.

Special considerations for the conduction heat transfer within the wafer include the temperature-dependent thermal properties of the material, the occurrence of phase change within the silicon layer, the microscale heat transfer effects of the thin films, and the effects of patterning on the surface. These phenomena must be addressed in an accurate analysis of the process. Research in this field has been limited, especially for graphite strip processing conditions.

The thermal conductivity of silicon, k, varies as a function of temperature as

$$k = \frac{299.0}{(T + 174.0)} \text{ W/cm °C} \qquad [2]$$

where T is the material's temperature in °C.[5] This expression is valid for temperatures below the melting point of silicon. When solid silicon reaches the melting point of 1412°C, the thermal conductivity is 0.1885 W/cm °C. Upon melting, the thermal conductivity increases drastically from 0.1885 to ~0.6 W/cm °C.[6,7] The results of a transient numerical model accounting for this temperature dependence were compared to the results of a constant thermal conductivity model. The comparison indicated that the error induced was negligible within the temperature domain during ZMR processing when a constant value was assumed as opposed to a value dependent on temperature.[8]

The thicknesses of the films are on the order of microns; consequently, the effect of their thermal resistance is small except for the case when large gradients are present. Due to the large thermal gradients within the film imposed by a high laser intensity, the thermal resistances are important considerations during laser heating analyses. In graphite-strip heating processes, the thermal gradients are much smaller than for laser processing, and the thermal resistance effect of the thin films becomes negligible.[8] Thus, for studies on the overall temperature profile during processing, numerical models of graphite-strip heating involving multilayer thin films can neglect the effect of the films thermal resistance. Nevertheless, there are optical considerations to take into account with the multilayer structure which will be discussed in a separate section of this paper.

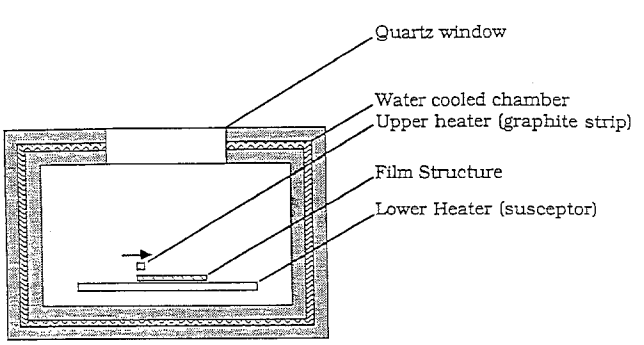

Fig. 3. Schematic of ZMR processing chamber.

At the microscale level, the heat absorbed into the structure was considered.[8] In actuality, the incident radiation penetrates the surface and continues into the wafer. This electromagnetic radiation attenuates as it travels further because the material absorbs some of this energy. It was found that minimal error was introduced by assuming total absorption at the surface.

The wafers can be patterned for the purpose of controlling the temperature profiles and recrystallization. Scribing through the insulating oxide creates a relief-patterned surface where the silicon recrystallizes as a single crystal.[9] Another technique to control the solidification front includes laying down strips of optical reflectors or absorbers in the scan direction which will affect the local temperature profile.[10] The solidification front morphology is forced into a desired shape, and the defects are generated at prescribed locations. A numerical study predicting the thermal effects of patterning was presented by Miaoulis and Mikic.[11]

Phase Change

Phase change during processing significantly affects the temperature distribution. Associated with the change in phase is a change in physical properties. Upon melting, silicon's thermal conductivity increases from ~0.2 to ~0.6 W/cm °C,[6] the bulk reflectivity increases from ~0.4 to 0.7,[12] and the emissivity decreases from ~0.6[13] to ~0.2.[14] The effects of other property changes such as density and specific heat have not been investigated yet. Although the heat source is a parallelepiped, the liquid/solid interface is not always planar. The morphology and stability of the interface change depending on the processing conditions. Because of the complexities associated, this phenomenon will be discussed separately in the section on Thermally Driven Instabilities at the Interface.

Numerical investigations of phase change during ZMR processing have implemented an enthalpy method to avoid the complexities with the stability of the interface. The algorithm which incorporates the enthalpy method and takes into account the nonplanar interface morphology is described below. Applications of the enthalpy method have been reported for laser scanning[15] and also for graphite-strip processing.[8]

The enthalpy method assumes that a specific control volume (numerical element) has a specific amount of enthalpy content. Thus, under melting conditions the amount of enthalpy in a control volume, H_{cv}, is

$$H_{cv} \le H_s = \int_0^{T_{mp}} (C_p) dT \qquad [3]$$

and when the material in the control volume is completely liquid, H_{cv} can be expressed as

$$H_{cv} \ge H_l = \int_0^{T_{mp}} (C_p) dT + \Delta H_f \qquad [4]$$

where H_{cv} is the enthalpy of the control volume per unit mass, H_s is the enthalpy of the solid silicon at the melting temperature per unit mass, H_l is the enthalpy of liquid silicon at the melting temperature per unit mass, C_p is the specific heat of silicon, ΔH_f is the heat of fusion of silicon per unit mass, and T_{mp} is the melting point of silicon. When

the enthalpy of the control volume has a value in between H_s and H_l

$$H_s < H_{cv} < H_l \quad [5]$$

the control volume is neither completely liquid nor solid. It is a mixture of solid and liquid material which is at the melting point temperature. At this solid-liquid transition, when the control volume's enthalpy has not reached the heat of fusion, the reflectivity, emissivity, and thermal conductivity of the control volumes are taken as the weighted average values of the properties for the solid and the liquid material, based on the enthalpy of the control volumes. When the material in a control volume starts changing phase, there will be a percentage of liquid material and a percentage of solid material. These percentages are linearly dependent on the average enthalpy in the control volume. The average thermal and optical properties of a control volume can then be obtained by a linear interpolation based on the enthalpy of the control volume. The property in question, β, at the control volume is defined as

$$\beta_{node} = \begin{cases} \beta_s & \text{for } H_{node} < H_s^{mp} \\ \beta_s + (\beta_l - \beta_s)\left[\dfrac{H_{node} - H_s^{mp}}{\Delta H_f}\right] & \text{for } H_s^{mp} < H_{node} < H_l^{mp} \\ \beta_l & \text{for } H_l^{mp} < H_{node} \end{cases} \quad [6]$$

where the "s" and "l" subscripts denote the solid and liquid phase property. H_s^{mp} is the enthalpy of the control volume when fusion starts, but all the material is still solid, and H_l^{mp} is the enthalpy of the control volume when fusion ends, but the liquid is still at the melting point temperature. The treatment above allows for a smooth transition for the reflectivity, emissivity, and thermal conductivity from solid to liquid values. Im *et al.* studied the effects of the optical property changes on the morphology of the melt zone.[3]

Radiation Effects

Major factors in the processing of films are the shape of the radiation intensity profile and the temperature of the infrared heat source.[18] There is also radiative cooling that takes place between the film structure and the surroundings, which is dependent on their temperature and radiative properties. We refer to these "bulk" radiation effects as macroscale radiation effects. Although there is always interaction on a microscopic scale, these macroscale radiation effects are dominated by the large scale parameters such as strip heater dimensions rather than the relatively smaller scale of film thicknesses. Since the thickness of the films is on the order of magnitude of the wavelengths of the infrared radiation, the radiative properties depend on the thickness and layering schemes in the multilayer film structure. We refer to these effects as microscale radiation effects. It is important to note that these radiative properties and effects can influence the stability of the solid/liquid interface during processing. These interface issues will be covered in the last section of this paper.

Macroscale radiation effects.—The radiation intensity profile depends upon the dimensions of the strip heater, and the distance of the strip heater to the wafer. Until Chen *et al.*[17] accurately described the intensity profile, a flat profile or Gaussian shape was assumed. Lipman *et al.*[18] evaluated the effects of the width and height of the strip heater and the distance between the strip heater to the wafer on temperature profiles and melt zone width. During the numerical experiments the strip heater was kept stationary at the centerline of the film structure, and the temperature distribution was recorded when the system reached steady state. They concluded that the width of the melt zone and the temperature gradients can be controlled effectively by varying these parameters. The width of the melt zone was influenced more by the width of the heat source than its height. If the distance between the strip heater and the wafer is increased, the radiation input profile becomes wider. This reduces the temperature gradients within the film, including those at the solid/liquid interface.

Other macroscale radiation effects to consider are the susceptor heating[19,20] and the ambient reflectivity effects. The bottom susceptor heater can strongly influence the temperature of the wafer. As the susceptor heating increases, the line heater intensity must be decreased. Im *et al.*[19] investigated the resulting change from reflective dominated effects to emissive dominated effects with increasing susceptor temperature. Explosive melting was observed as the susceptor heating increases. For lamp heating experiments, Dutartre[20] found that low susceptor heating produced better quality crystals than high susceptor heating.

The ambient reflectivity of the chamber may also influence the background heating. Radiative cooling from the wafer may be reflected from the ambient reflectivity which will heat the wafer. The interaction of the ambient reflectivity is currently being investigated in our laboratory.

Microscale radiation effects.—Electromagnetic radiation generated by the heat source incident on the multilayer film structure will be partially reflected and transmitted at each film interface (see Fig. 4). Since the wavelengths of the thermal radiation are on the order of magnitude of the film thicknesses, considerable interference of the electromagnetic radiation will occur within the multilayers. Reflectivity from the surface of the wafer is influenced by the interference within the structure. A change in the thickness of a film will alter the interference within the layers and the resulting net reflectivity. Therefore, the amount of heat absorbed by the structure is determined by the dimensions of the films on the substrate.

Several studies have been conducted with regard to laser annealing and infrared source heating which incorporate these optical effects. Indeed, microscale radiation effects were investigated for laser heating before infrared heating. In this section the work done in laser heating as well as in infrared heating are presented since there are similarities between the two cases. There are also differences between the use of the two heat sources. The infrared heater is different from the laser in two main ways: (*i*) the laser is a more intense, concentrated heat source, whereas the infrared heat source heats a larger region of the surface, and (*ii*) the laser emits at a single wavelength, whereas the infrared source emits a range of wavelengths. The angular dependency of the radiation must also be considered in infrared heating. Thin film optics can be applied to an analysis of these thin film structures exposed to laser heating. Several researchers have used the techniques described by Heavens,[21] Born and Wolfe,[22] and Knittl.[23] For infrared heating, the radiative properties can be calculated by weighing and integrating over the thermal radiation spectrum.[24] After obtaining the radiative properties of the multilayer structure, it is desirable to obtain information on the temperature profiles and the molten region size.

Radiative properties.—Although the focus of this paper is on infrared heating, there has been considerable work done in microscale radiation effects due to laser heating. These results can be applied to infrared processing as well, in particular the optical properties at high temperatures. It should be noted that the optical properties of materials are functions of both wavelength and temperature. For laser heating, the radiative properties, transmissivity, absorptivity, and reflectivity of the thin film multilayer structures have been examined by several investigators. As expected, a periodic relationship exists between the radiative property and film thickness. One of the first studies conducted on the optical effects of thin films was that of Tamura *et al.*,[25] in which the behavior of a silicon substrate capped with a thin SiO_2 film during laser annealing was investigated. The effects of varying the SiO_2 film thickness on transmissivity into the substrate was examined using a general equation for transmissivity of a single layer.[22] A periodic relationship was found between film thickness

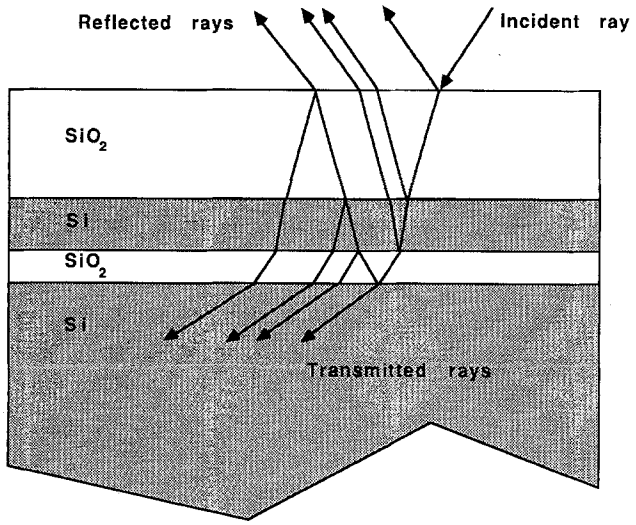

Fig. 4. Optical ray path through SOI wafer.

and transmissivity which agreed with experimental data. A numerical model employing the matrix method was developed by Colinge and Wiele[26] to determine the laser power absorbed in a SOI structure while taking into account the optical effects of the thin films. The effects of changing oxide thickness on the absorbed power in the polysilicon film were described for different wavelengths of an argon laser and also for an argon laser in the multi-line mode. In each case, a sinusoidal relationship was observed. The results obtained were compared to a semi-quantitative study, in which samples were annealed with various incident powers. The samples were then observed under a microscope and the degree of melting traces correlated to the amount of power absorbed. There was good agreement between experimental and numerical results.

The numerical model developed by Wong *et al.*[24] involved the use of a graphite-strip heating of a SiO_2 capped SOI wafer. With constant optical properties, parametric studies were conducted below the melting temperature in which each of the three film thicknesses were independently varied from 0.5-2.0 μm while the others were kept constant. The reflectivity profiles across the surface were different for each film thickness (Fig. 5). In the figure, the four reflectivity profiles are for four different layering schemes delineated by capping oxide film thickness, silicon film thickness, insulating oxide film thickness; all thicknesses are in microns. The changes were not linear as the thickness increased. Wavelength-dependent optical properties were considered in another analysis for infrared heating.[27] Results indicated that although the absolute values obtained were different, the same trends occurred in both cases.

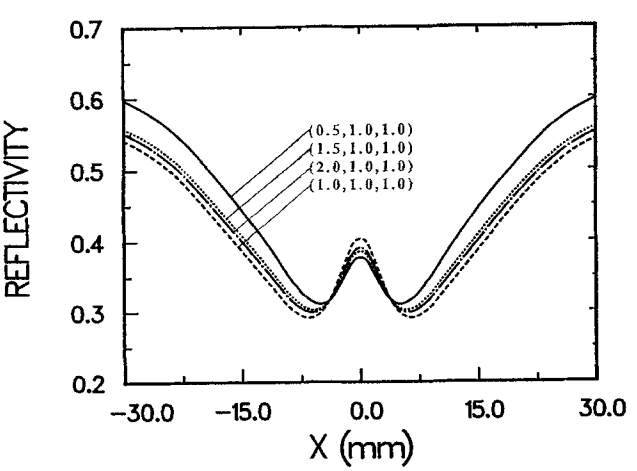

Fig. 5. Effect of capping silicon oxide film thickness on the reflectivity across the surface.

Because of the large range of temperatures involved in silicon processing, the temperature-dependent optical properties of silicon are needed for an accurate analysis. Temperature profiles were calculated from a numerical model of a scanning laser in a semi-infinite material by Moody and Hendel.[28] In their calculations, reflectivity was taken as a function of temperature. It was shown that this method, as opposed to taking a constant reflectivity, reduced the maximum material temperature in the center of the beam spot by approximately 10%. Grigoropoulos *et al.*[15] have also investigated the effects of temperature on the optical properties. Reflectivity, absorptivity, and transmissivity were calculated as a function of temperature for a specific layering scheme. Optical properties were taken from the works of Jellison and Burke,[29] Jellison,[30] and Shvarev *et al.*[14] The emissivity as a function of temperature was also determined for the structure.

Temperature profiles and melt sizes.—The radiative properties are important for analyses of the temperature profiles and molten region sizes which are needed to examine the microscale radiation effects more effectively. Calder and Sue[31] developed a general algorithm for determining the temperature profiles during laser annealing of multilayer structures at steady state with no melting. The two-layer structure (Si/SiO_2) and three-layer structure ($Si/SiO_2/Si$) were numerically studied. Temperature profiles were then calculated for varying the Si film thickness for the two-layer structure and oxide film thicknesses for the three-layer structure. For the two-layer case, a study was conducted to measure the error in surface temperature between their model and a cruder model in which all energy was absorbed at the surface. The errors became significant as the thickness increased. Grigoropoulos *et al.*[15] developed a 3-D numerical model of a ($SiO_2/Si/SiO_2$) substrate which includes melting by employing the enthalpy method. Temperature distributions were then calculated with a finite difference numerical algorithm. The numerical results compared well with the experimental results. To avoid the need to obtain optical property data at high temperatures, a semiempirical model was developed by Willems *et al.*[32] in order to determine the melting threshold power for the laser-induced molten zone in a scanned laser recrystallization process. Expressions were derived using the observed melt width as a function of different processing conditions. Then the matrix method was used to calculate the optical interference within the thin films. The results of these calculations were fit to the experimental expressions used in predicting the power needed to melt the silicon for new SOI structures. They concluded that the effects of the underlying oxide film on the amount of absorbed power is minimal. However, the temperature dependency of the absorption coefficient was important, since the absorption coefficient increased exponentially with temperature.[33]

For the infrared heating analysis by Wong *et al.*,[24] the calculated reflectivity profiles were used to calculate the temperature profiles. Changes in the capping and insulating layers resulted in nonlinear changes in temperature, while changes in the silicon layer resulted in a nearly linear change in temperature. The maximum temperature reached directly under the strip was determined as a function of each layer thickness. For the capping layer, a relative minimum occurred at a thickness of 1 μm (Fig. 6). A slight increase or decrease in thickness would raise the maximum temperature about 10°C. For the insulating layer, a relative minimum was also reached at 1.0 μm, where temperatures increased slightly above and below this thickness. The results of this study identified the equal film thicknesses layering scheme as especially sensitive to changes in thickness.

The model by Wong *et al.* was modified to include melting and similar results were found.[34] In this case, the reflectivity profile directly under the strip increased due to the highly reflective nature of silicon in the liquid state. The temperature profile for varying capping layer thicknesses from 0.5 to 2.0 μm was calculated, and the melt width was found to vary nonlinearly within a range of 750 to 1050 μm.

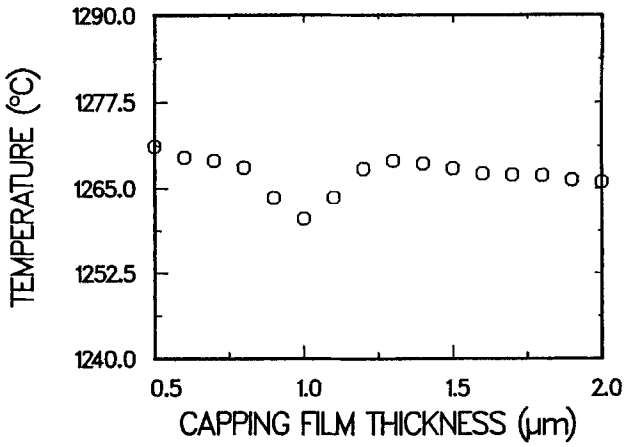

Fig. 6. Effect of capping silicon oxide film thickness on the maximum temperature attained.

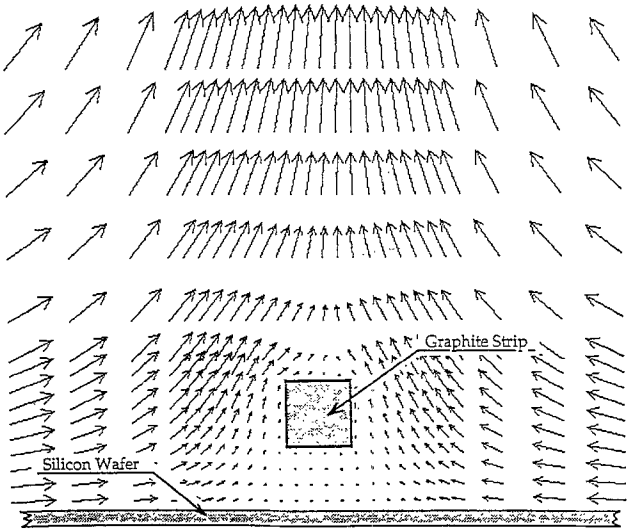

Fig. 7. Gas flow velocity field inside sealed chamber during typical ZMR processing conditions.

Again, the equal film thicknesses layering scheme was found to be sensitive. The effects of varying film thicknesses on temperature and on the structure of the melt zone region were again described for wavelength dependent optical properties.[27] Effects of each film thickness were compared to the width of the slush region, liquid region, and the total melt zone width. The slush width is related to the structure of the solidification interface morphology.[35] However, similar slush melt zone widths may not contain the same proportions of solid and liquid and do not necessarily result in the same crystal quality.

In these infrared heating studies, a reflectivity maximum was observed with the equal oxide thickness schemes. It was speculated that this is due to a radiation cross-correlation phenomenon.[36] When the optical thickness of the first oxide film is equal to the optical thickness of the second oxide film, an integration over the broad spectrum will cause a cross-correlation effect to occur. The temperature dependence of the index of refraction will not significantly alter the cross correlation results since the optical thicknesses of both oxide films will change together.

It is evident that the microscale radiation effects in thin film processing with an infrared heat source should be taken into account for an accurate analysis. The reflectivity and other radiative properties may vary nonlinearly with film structure properties and thicknesses. Moreover, there are several remaining questions about the optical effects of the multilayer thin films that remain to be investigated. To obtain accurate results, the models developed must incorporate accurate property values at elevated temperatures. The data base for silicon, silicon oxide, and other electronic materials used in thin films is quite limited. The current data available is applicable only for a small range of wavelengths and temperatures. Because of the sensitivity of the temperature profiles to a slight change in film thickness, any perturbation on the surface may cause significant effects. The slight change in the local optical properties due to these small structures in the multilayer structure could have an effect on the solidification front morphology and resultant quality. This phenomenon is currently under investigation in our laboratory. The optical effect of the multilayer structure should also be investigated for the case of quartz lamp heating which emits discrete wavelengths. The elliptical mirror's shape requires angular considerations to be taken into account for accurate analysis; the range of incident angles is more important in this case than in graphite strip heating which involves a small cross-sectional heater. Whether or not the cross-correlation effect exists for quartz lamp heating is presently unknown.

Convective Cooling Effects

During ZMR, the processing chamber is often flushed with a gas such as argon or helium to provide an inert atmosphere for zone-melting since oxygen will attack the heated graphite and damage the strip heater.[37] It is essential to determine whether convective heat loss induced by the moving gas currents in the chamber is a significant factor in the temperature profile and the melt width of the film structure. The only study that reported the effects of convection during radiant processing of films is by Miaoulis *et al.*[9] This study focused on natural and forced convection effects on the temperature distribution within the film. For both cases the film structure was modeled as a flat plate, and convection coefficients were obtained for a variety of conditions. The heat transfer coefficients were implemented into the numerical simulation of ZMR.[9] When convective effects were incorporated to obtain temperature profiles in the film during processing, a melt-zone width decrease due to convection was observed. By introducing argon into the chamber, the melt zone would shrink by 10% and by introducing helium by 19% for natural convection conditions. Although these results are approximate, they demonstrate the sensitivity of the melt zone width to different inert gas atmospheres. Similar effects were observed for forced convection conditions.

Modeling the system as a flat plate provides some insight into the effects of convection but does not offer an accurate prediction of the size of the melt zone width. Recent numerical (using PHOENICS software) and flow visualization studies performed in our laboratory, indicated that there is a region underneath the heat source where natural convection is suppressed (Fig. 7). The flat-plate assumption does not take this effect into consideration. We are currently evaluating the local convective coefficients on the film. These coefficients in the analysis can provide us with a more accurate evaluation of the processing chamber convection effects.

Velocity Effects

In this section, the effect of velocity on the temperature profile, melt width, and thermal gradients are described. The benefits and problems associated with increasing velocity are also covered. Although supercooling effects are closely related to scan speed, these issues will be presented in the section on Supercooling on ZMR.

Temperature profiles and melt sizes.—The motion of the heat source skews the temperature profiles, reduces the thermal gradient at the solidification interface, lowers the maximum temperature attained, and alters the molten zone. In numerical studies, Yoon and Miaoulis[38] evaluated the effect of scan speed on the changes in temperature profiles and melt widths. The motion of the strip heater was numerically simulated by redistributing the heat sources along the surface transiently. The shifting effect on the molten region due to strip motion is shown in Fig. 8. A stationary profile is contrasted with a profile at a typical

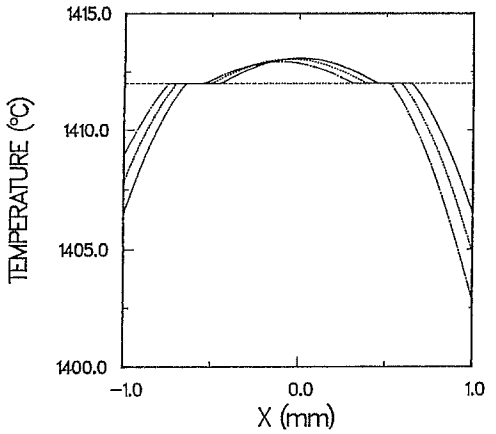

Fig. 8. Effect of scan speed [V = 0 μm/s (——), v = 300 μm/s (···), and v = 600 μm/s (—·—)] on the temperature profile underneath the strip.

processing speed of 300 μm/s and a higher speed of 600 μm/s. This lag generated by increasing the scan speed, occurs because the material downstream from the strip heater has less time to cool (radiatively and conductively), while the material upstream has less time to absorb heat. This shift of the molten region indicates the importance of accounting for scan speed when modeling the ZMR process. The magnitude of radiation intensity varies as a function of position below the strip heater[18] so that modeling the heat source as stationary may not be capturing the correct intensity profile. Results from their parametric study indicate that the maximum temperature achieved during ZMR was not affected for scanning speeds below 400 μm/s. The size of the molten region was also affected by scanning speed. In Fig. 9, it is evident that the scanning speed did not affect the length of the molten region until a velocity of 400 μm/s after which the molten region shrank.

These changes in the temperature profiles with increasing scan speed will, in turn, change the morphology of the solid/liquid interface and the resultant quality of the material. There are many problems associated with high scan speed processing such as incomplete melting[11,39,40] of the material and unstable solidification morphologies which affect the defect density.[40,42] In fact, there appears to be a limiting scan speed above which the resultant crystalline quality drops dramatically.

Conditions for complete melting.—Analytical, experimental, and numerical work have been conducted to find the processing conditions which will insure complete melting. Analytical work by Miaoulis and Mikic[9] for a two-dimensional heat source moving over a flat plate, whose bottom surface is kept at constant temperature, determined the power requirements for the heat source to insure melting for increasing velocities. Pfeiffer *et al.*[39] proposed that the scanning speed only needed to be kept below 500 μm/s for there to be sufficient time to completely melt all the polycrystalline feedstock. A numerical study performed by Lipman[40] determined the minimum temperature of the graphite strip heater needed to melt the silicon film for different scanning velocities. They found that for speeds of up to 300 μm/s, the needed increase in strip temperature was negligible. They also determined the required temperature for higher speeds.

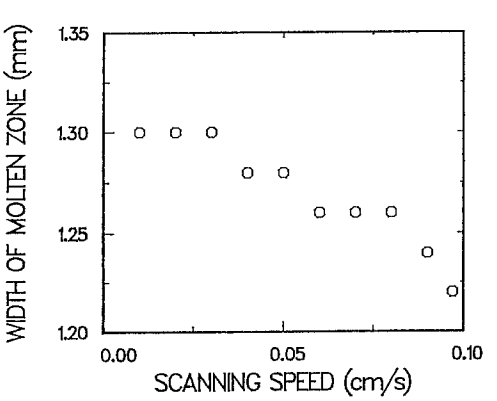

Fig. 9. Effect of scan speed on width of molten zone.

Thermal gradients and crystalline quality.—It has been observed experimentally that the quality of the films can be increased if the thermal gradients at the solidification interface can be reduced. Pfeiffer *et al.*[41] studied experimentally the effect of different scanning speeds and prescribed thermal gradients during graphite strip heater recrystallization of SOI structures. For lower velocities (<300 μm/s) and reduced thermal gradients, they obtained higher quality films which contained only threading dislocations, instead of edge dislocations which could run the distance of the film. The spacing between dislocations became greater for smaller thermal gradients which were induced by higher scanning speeds. However, the scan speed can be increased only up to a certain limit after which the residence time is too short for complete melting of the silicon film.

Im *et al.*[42] studied the morphology of the crystallization front during graphite strip ZMR with a graphite strip power of 2.5 kW. For scan speeds below 350 μm/s, increasing the scanning velocity caused the spacing between cells to increase, which was consistent with the work done by Pfeiffer *et al.*[41] The increasing velocity also caused the depths of the cusps to deepen and isolated dislocations and dislocation clusters were observed. When the velocity increased above 350 μm/s, the morphology of the liquid/solid interface became unstable, and densely packed dislocation clusters as well as continuous-edge dislocations, or subboundaries, were observed.

In summary, an increase in scan speed can affect the thermal gradients at the solidification interface, the minimum power requirement to insure complete melting, the structure of the molten zone, and the quality of the resultant crystal. These thermal issues can be typically neglected for low scan speeds (~350 μm/s) depending on the other processing conditions.

Supercooling in ZMR

A phenomenon which influences the morphology of the solidification interface and temperature profiles in the film during ZMR processing is constitutional supercooling. Impurities introduced during ZMR will be pushed by the solidification front during crystallization[42] resulting in concentration of impurities in the liquid region. This concentration of impurities causes a depression of the freezing point.[43-45] The freezing point of the melt will be depressed to temperature T_f given by

$$T_f = T_m + mc \qquad [7]$$

where T_m is the melting point of pure silicon, m is the slope of the liquidus line on the phase diagram of silicon and the impurity, and c is the concentration of the impurity in the silicon film. If the temperature of the liquid in front of the interface is below the equilibrium liquidus temperature, constitutional supercooling occurs.[46,47] There is experimental evidence that impurities are present during the ZMR process and that constitutional supercooling may be responsible for a nonplanar liquid/solid interface which is a precursor to subboundary formation.[48]

Impurity concentrations.—There is evidence that impurities from the neighboring thin films and in the processing chamber are present in the silicon film during processing. Fan *et al.*[49] found oxygen concentrated in the subboundaries during their research on graphite strip heater ZMR of SOI structures. They suggest that the oxygen had dissolved from the encapsulating layer into the molten silicon. Concentrations of carbon and oxygen around 10^{17}-10^{18} atm/cm^3 were found in their investigation. Mertens *et al.*[50]

found oxygen and nitrogen saturated in the silicon film. They found oxygen concentrations of 2×10^{18} atm/cm^3 and nitrogen concentrations of 6×10^{18} atm/cm^3 as well as a liquidus slope of -8×10^{-21} °C cm^3 for Si-N in ZMR processed silicon films. They also concluded that these impurities emanated from a capping layer of SiH_4 and N_2O, since the dissolution time of nitrogen and oxygen into silicon was less than the dwell time of the molten zone.

Temperature profiles and melt widths.—The effect of constitutional supercooling on both the molten region and freezing slush zone for scanning speeds up to 1000 μm/s was studied in our laboratory.[38] The numerical model was developed to simulated motion by redistributing the heat sources along the surface transiently and accounted for the supercooling by numerically changing the freezing point in the enthalpy method. Our numerical studies examined different amounts of supercooling up to 5°C, which could occur for large impurity segregation at the interface. The values for m: −148°C/atom percent (a/o) for Si-O and 16°C/a/o for Si-C were approximated from phase diagrams.[51-53] The distribution of the impurities and the degree of supercooling varies throughout the slush region because the impurities are concentrated in the cusps between cells.[46] An average amount of supercooling was represented in our analysis.[38] For a given velocity and degree of supercooling, the numerical model calculated the temperature distributions within the film. Results indicated that constitutional supercooling had a significant effect on the temperature profiles during ZMR. In Fig. 10, a case with no supercooling at 500 μm/s is compared with cases of 2 and 5°C of supercooling. These temperature profiles were not symmetric about the position of maximum temperature and the total length of the molten zone increased with a greater amount of supercooling. Also, the size of the freezing slush region decreased with a greater amount of supercooling. Because more cooling was necessary to reach a depressed freezing temperature, the temperature gradient will be steeper than the case without supercooling and the slush region will be reduced. In general, for a constant scanning speed, the molten region grows for increasing amounts of supercooling. When supercooling is present the melt does not crystallize as quickly because more radiative cooling is needed for the temperature of the melt to reach the depressed freezing temperature. If the amount of supercooling was held constant and the scanning speed was varied, the melt width and the size of the slush region were not affected by increasing velocities up to 400 μm/s.

Instability of interface.—In the above analysis, the changes in temperature profiles were described when supercooling was present. However, the interface morphology and its stability cannot be determined from those results. In fact, many investigators have suggested that constitutional supercooling is also responsible for the

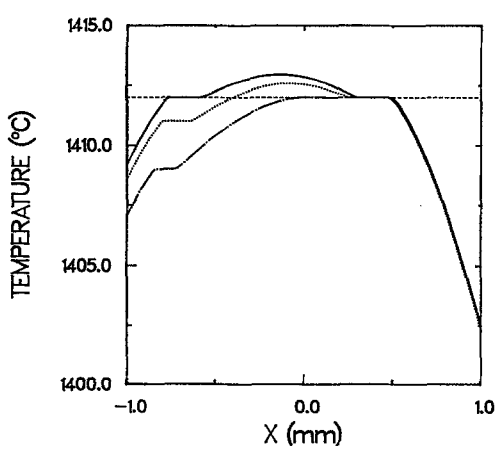

Fig. 10. Effect of amount of supercooling [ΔT_{sc} = 0° (——), ΔT_{sc} = 2° (···), and ΔT_{sc} = 5° (—·—)] on the temperature profile underneath the strip.

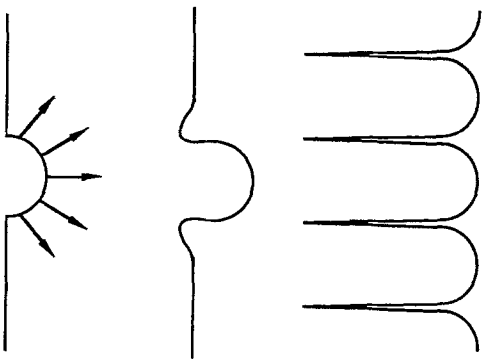

Fig. 11. Schematic of the transition of the planar interface to a cellular one.

faceting[49] and interfacial instability during ZMR.[47,48,54] Lee investigated energy-beam recrystallization of SOI structures, concluding that the breakdown of the solidification front was from constitutional supercooling.[48] Work done on ZMR of SOI wafers using a halogen lamp showed that the instability of the interface was most likely caused by impurity segregation according to Dutartre *et al.*[54] In the last section, we discuss other sources of thermal instabilities which are more probable causes of interface instability.

In general, if an impurity is present, solute diffusion must be coupled with thermal diffusion to determine crystal growth. For impure melts, the solute ahead of the solidification interface depresses the freezing point. The planar interface becomes unstable because it is exposed to a gradient of supercooling. The formation of the cellular interface from planar can be seen schematically in Fig. 11. The unstable region would grow as a perturbance until its convexity and rejection of solute provided enough driving force for growth. A cellular morphology of the advancing interface results because convexity at the sides of one perturbance will trigger other perturbances around it. Solute rejection into cusps between cells retards the growth between cells.[44] The role of supercooling in the stability of the solidification interface is still being investigated for ZMR processing.

Sub-boundary formation.—Since Fan *et al.*[49] found oxygen in the sub-boundaries, they believe that sub-boundary formation was due to constitutional supercooling. Leamy *et al.*[47] and Lee[48] have also found impurities in the sub-boundaries during ZMR studies. It is well known that during constitutional supercooling impurities will concentrate in the cusps of the cellular or dendritic formation.[46] This implies that the sub-boundaries grow from the cusps of the cellular interface. The elimination of sub-boundaries therefore requires further study of the effect of impurities, supercooling, and thermal stresses in ZMR.

Thermally Driven Instabilities at the Interface

The solidification interface morphology plays the most important role in determining the quality of the post-processed material. It is commonly understood that defect trails and sub-boundaries form at the interior corners of faceted fronts and at the cusps of cellular fronts (see the section on Sub-boundary formation). Contrary to intuition, the solidification front morphology is not always planar. Several investigators[3,42,55] have made *in situ* observations of cellular, dendritic, or faceted interfaces. The lowest defect densities have been produced after processing with a cellular interface.[3] Figure 11 shows a sketch of a transition of a cellular interface from a planar one. Dutartre[55] used a laser and a lamp source to observe the *in situ* solidification growth. He varied the thickness of the samples and the scan speed and left previous grain boundaries and sub-boundaries in the wafer to observe the effect on the solidification front morphology. Limanov and Givargizov[56] used a laser heat source to study the solidification front morphology. The need to know the shape and stability of the interface have lead investigators to construct several

different physical models. These models describe different phenomena as being responsible for the interface stability (note: supercooling as an instability was covered in the section on Instability of interface and will be discussed further here).

Faceted growth model.—The archetype of the faceted growth model was proposed by Geis *et al.*[4] in 1983. Their experimental investigation used a graphite strip heater and a grating of optical absorption strips deposited on the SOI wafer. The Si material beneath the strips remained at a higher temperature than the uncovered Si, allowing the uncovered portion of the Si to freeze first. The spacing of the facets, and thereby the sub-boundaries, was controlled in this manner; however, they were only able to obtain *ex situ* observations. In their faceting model the film was assumed to have the scan direction proceed along the <100> direction of the (100) textured film. Faceted growth was accomplished by the addition of atoms at the ledges or facet corners. The facets were assumed to grow along the solid/liquid interface at (111) planes, which was normal to the substrate plane. Based on the model for faceted interface morphology developed by Geis *et al.*,[4] Pfeiffer *et al.*[57] examined quantitatively the development of the sub-boundaries. Their numerical model related the growth rate of a facet to its length and position with respect to the melting isotherm line.

A few years later, different investigators presented *in situ* observations as verification of facet growth. *In situ* observations of lamp zone melting were done by Dutartre[9] and Dutartre *et al.*[58] An etched-patterned thermally oxidized Si wafer was used as the substrate for the polycrystalline Si film. Scan speeds were varied to observe the changes in both the morphology and defect structures. As scan speed was increased, the tips of the cells appeared to become sharper. This appeared to be an indication of a transition to facet structures. Experimental and theoretical studies of the faceting solid-liquid interface were also performed by Arnold *et al.*[59] Using a laser in their experimental work they examined the equilibrium solid-liquid structures that exist in a molten zone. Through *in situ* observations, they concluded that the solidification morphology changes from cellular to faceted as steady state was reached. A molecular dynamic model was used to numerically analyze the equilibrium and non-equilibrium microscopic structures in this molten zone. The model solves the equations of motion for interacting particles. Two-body and three-body interatomic energy potentials were used and optimized to replicate several crystalline and mechanical properties of silicon. The equilibrium structure of the solidification front showed that the interface consisted of alternating (111) and ($\bar{1}11$) facet planes.

The facet model was also used to explain the relation between thermal gradients and crystalline defects by Pfeiffer *et al.*[39] and Pfeiffer *et al.*[2] The freezing profile with respect to the film thickness was incorporated into the faceted model. At the interior corners of the facets, the solid/liquid interface was proposed to be normal to the substrate plane for high thermal gradients (~10 K^0/mm). However, for low thermal gradients (~4 K^0/mm) the interface tilted towards the plane of the SiO_2 film. Moreover, defects were described as growing normal to the interface plane. This implied that lower thermal gradients would produce more localized defects rather than the continuous-trail defects associated with high thermal gradient processing.

While the facet model has made a significant contribution to crystal growth theory in ZMR, it cannot singularly be used to describe the solidification interface dynamics and the resulting defect trails. Its most important contribution is the incorporation of orientational growth in silicon (*i.e.*, fast and slow growth planes). Indeed the tendency of certain growth planes in silicon to grow faster than others should figure into the interfacial growth dynamics. But it does not sufficiently explain the variations in sub-grain boundary spacing with film thickness, and the formation and existence of re-entrant corners.[55] The effect of impurities and the change in optical properties of silicon are equally, if not more, important than orientational growth in determining the solidification front morphologies, and should be further examined (see next section) before a complete theory can be developed.

Changes in radiative properties.—Investigators have examined other effects which could be responsible for the instability of the interface. The earliest studies on the effect of the changes in radiative properties between solid and liquid phases have been for laser heating ZMR. Jackson and Kurtze studied the stability of solid and liquid alternating lamellae in silicon films induced during laser beam heating[12] using a Mullins and Sekerka instability analysis.[45] The analysis accounted for the reflectivity difference between the solid and liquid phases of silicon (see the section on Phase Change). The results indicated that perturbation growth created subdivisions of the solid and liquid until the period was small enough to be stable. Grigoropoulos *et al.*[60,61] conducted two studies on instabilities in laser-induced crystal growth on thin polysilicon layers. They found that the stability of the solid/liquid interface was affected by Gibbs-Thomson temperature boundary conditions and the abrupt change in reflectivity between solid and liquid silicon. In their experiments, a laser beam was scanned at constant velocity across a thin silicon layer deposited on a heat sink structure. They also used a Mullins and Sekerka linear perturbation analysis[45] to study the stability of the solidification front. They concluded that the change in reflectivity promoted instability; however, small amounts of supercooling and superheating could be tolerated without destabilizing the interface from stability contributions due to surface tension.

Radiatively induced cellular interface.—In studies for graphite strip heater ZMR processing, Im *et al.*[3,35] varied the power and height of the heater in order to observe cellular-dendritic,[3] cellular, faceted and various transition structures. Most importantly they studied the resulting morphology of a film when a previously moving strip was halted and held stationary with respect to the wafer. The cellular and cellular-dendritic interfacial structures persisted even while the strip was stationary. From the persistence of the morphology, they concluded that the effects of impurities had little to no influence on the stability of the interface, and thus constitutional supercooling was not the cause of the instability. An important alternate theory to explain these stationary protrusions stated that the spatial intensity gradient may be responsible for the interface structure.

A following study by Im *et al.*[42] varied the velocity and power of a graphite strip heater system to observe the morphology and resultant quality of the crystal. For increasing power to the strip heater, the period of the cells decreased and the types of defects changed. Another study was done to observe the effects for increasing velocity. Results indicated that cell period increased for low velocities and then decreased for high velocities. The increase in cell period for low velocities opposed conventional supercooling theory on cell spacing. This was another indication, along with the persistence of stationary cells, that supercooling is not responsible for the interface instability for low velocities. Complementing this experimental work on the cell period, Im[62] conducted an instability analysis of solid and liquid lamellae. He obtained good agreement between experimental and analytical results.

Summary.—It is most likely that not one single influence exclusively controls the solidification dynamics of any system. It is a variety of effects that, when summed, produce the observed pattern. The most influential factor for the solidification front morphology is the change in optical properties from the solid state to the liquid state. Supercooling may affect the defect generation during processing and also play a role in altering the stability for higher velocities. In a review, Dutartre[55] collects differing opinions on the major solidification dynamics influences. He also

concludes that the solidification morphology is due to a variety of frontal breakdown phenomena.

Conclusions

An overview of the thermal issues in ZMR processing of SOI structures with an infrared line heat source has been presented. Investigators have found that the crystal growth strongly depends on the control of the temperature profile, melt width, and solidification interface morphology. High quality films can be produced with various combinations of scan speeds and radiative heating conditions.

Radiation heat transfer and phase change effects were found to have large significance in the fundamental physics behind ZMR processing. The scanning speed, the amount of constitutional supercooling, and the stability of the solidification interface also play critical roles during such a process. These thermal issues must be investigated further in order to reduce the amount of defects in the crystal as well as other problems during processing.

Acknowledgments

The research conducted at the Tufts Thermal Analysis of Materials Processing Laboratory was funded by the National Science Foundation under grants MSM-8817949 and EID-9017557.

Manuscript submitted Jan. 6, 1992; revised manuscript received about May 18, 1992.

Tufts University assisted in meeting the publication costs of this article.

REFERENCES

1. I. N. Miaoulis, in *Proceedings of the Symposium on Recrystallization in Metallic Materials,* pp. 705-710, The Minerals, Metals and Materials Society, Warrendale, PA (1990).
2. L. Pfeiffer, A. E. Gelman, K. A. Jackson, K. W. West, and J. L. Batstone, *Appl. Phys. Lett.,* **51,** 1256 (1987).
3. J. S. Im, C. V. Thompson, and H. Tomita, in *Proceedings of the Symposium on Beam-Solid Interactions and Transient Processes,* Vol. 74, pp. 555-560, Materials Research Society (1987).
4. M. W. Geis, H. I. Smith, D. J. Silversmith, and R. W. Mountain, *This Journal,* **130,** 1178 (1983).
5. C. P. Grigoropoulos, R. H. Buckholz, and G. A. Domoto, *J. Appl. Phys.,* **60,** 2304 (1986).
6. L. O. Wilson and G. K. Celler, in *Proceedings of the Symposium on Energy Beam-Solid Interactions and Transient Thermal Processing,* Vol. 35, p. 623, Materials Research Society (1985).
7. Yu. H. Shahkov and V. P. Grishin, *Sov. Phys. Solid State,* **8,** 447 (1966).
8. I. N. Miaoulis, P. Y. Wong, J. D. Lipman, and J. S. Im, *J. Appl. Phys.,* **69,** 7273 (1991).
9. D. Dutartre, *Appl. Phys. Lett.,* **48,** 350 (1986).
10. J. P. Colinge, E. Demoulin, D. Bensahel, and G. Auvert, *ibid.,* **41,** 346 (1982).
11. I. N. Miaoulis and B. B. Mikic, *J. Appl. Phys.,* **59,** 1658 (1986).
12. K. A. Jackson and D. A. Kurtze, *J. Crystal Growth,* **71,** 385 (1985).
13. G. K. Celler, L. E. Trimble, and L. O. Wilson, in *Proceedings of the Symposium on Energy Beam-Solid Interactions and Transient Thermal Processing,* Vol. 35, p. 636, Materials Research Society (1985).
14. K. M. Shvarev, B. A. Baum, and P. V. Gel'd, *Sov. Phys. Solid State,* **16,** 2111 (1975).
15. C. P. Grigoropoulos, W. E. Dutcher, Jr., and A. F. Emery, *J. Heat Transfer,* **113,** 21 (1991).
16. B. V. Karlekar and R. M. Desmond, *Heat Transfer,* 2nd ed., p. 329, West Publishing, St. Paul, MN (1982).
17. C. K. Chen, M. W. Geis, B-Y. Tsaur, R. L. Chapman, and J. C. C. Fan, *This Journal,* **131,** 1707 (1984).
18. J. D. Lipman, P. Y. Wong, I. N. Miaoulis, and J. S. Im, *HTD Collected Papers in Heat Transfer,* Vol. 123, pp. 211-217, The American Society of Mechanical Engineers (1989).
19. J. S. Im, J. D. Lipman, I. N. Miaoulis, C. K. Chen, and C. V. Thompson, in *Proceedings of the Symposium on Beam-Solid Interactions: Physical Phenomena,* Vol. 157, pp. 455-460, Materials Research Society (1990).
20. D. Dutartre, *Mater. Sci. Eng.,* **B4,** 211 (1989).
21. A. S. Heavens, *Optical Properties of Thin Films,* pp. 66-74, Butterworths, London (1955).
22. M. Born and E. Wolf, *Principles of Optics,* Pergamon Press, Ltd., London (1970).
23. Z. Knittl, *Optics of Thin Films,* pp. 240-282, Wiley, Prague (1976).
24. P. Y. Wong, I. N. Miaoulis, and P. Zavracky, *DSC Microstructures, Sensors, and Actuators,* Vol. 19, p. 175-187, The American Society of Mechanical Engineers (1990).
25. H. Tamura, M. Miyao, and T. Tokuyama, *J. Appl. Phys.,* **50,** 3783 (1979).
26. J. P. Colinge and F. Van de Wiele, *ibid.,* **52,** 4769 (1981).
27. P. Y. Wong and I. N. Miaoulis, *ibid.,* **70,** 7594 (1991).
28. J. E. Moody and R. H. Hendel, *ibid.,* **53,** 4364 (1982).
29. G. E. Jellison, Jr., and H. H. Burke, *ibid.,* **60,** 841 (1986).
30. G. E. Jellison, Jr., *Semiconductors and Semimetals,* Vol. 23, R. F. Wood, C. W. White, and R. T. Young, Editors, pp. 95-164, Academic Press, Inc., Orlando, FL (1984).
31. I. D. Calder and R. Sue, *J. Appl. Phys.,* **53,** 7545 (1982).
32. G. J. Willems, J. J. Poortmans, and H. E. Maes, *ibid.,* **62,** 3408 (1987).
33. G. E. Jellison, Jr., and F. A. Modine, *Appl. Phys. Lett.,* **41,** 180 (1982).
34. P. Y. Wong, I. N. Miaoulis, and P. Zavracky, *Proceedings of the Symposium on Surface Chemistry and Beam Solid Interactions,* Vol. 201, Materials Research Society (1990).
35. J. S. Im, H. Tomita, and C. V. Thompson, *Appl. Phys. Lett.,* **51,** 685 (1987).
36. P. Y. Wong, L. M. Trefethen, and I. N. Miaoulis, *DSC-Microstructures, Sensors, and Actuators,* Vol. 32, pp. 349-359, The American Society of Mechanical Engineers (1991).
37. J. C. C. Fan, B.-Y. Tsaur, and M. W. Geis, *J. Crystal Growth,* **63,** 453 (1983).
38. S. M. Yoon and I. N. Miaoulis, *J. Mater. Res.,* Submitted for publication.
39. L. Pfeiffer, A. E. Gelman, K. A. Jackson, and K. W. West, *Proceedings of the Symposium on Beam-Solid Interactions and Transient Processes,* Vol. 74, pp. 543-553, Materials Research Society (1987).
40. J. Lipman, I. N. Miaoulis, and J. S. Im, in *Proceedings of the Symposium on Beam-Solid Interactions: Physical Phenomena,* Vol. 157, pp. 473-478, Materials Research Society (1990).
41. L. Pfeiffer, K. W. West, D. C. Joy, J. M. Gibson, and A. E. Gelman, in *Proceedings of the Symposium on Semiconductor-on-Insulator and Thin Film Transistor Technology,* Vol. 53, pp. 29-38, Materials Research Society (1986).
42. J. S. Im, C. K. Chen, C. V. Thompson, M. W. Geis, and H. Tomita, in *Proceedings of the Symposium on Silicon-on-Insulator and Buried Metals in Semiconductors,* Vol. 107, pp. 169-174, Materials Research Society (1988).
43. D. P. Woodruff, *The Solid-Liquid Interface,* p. 83, Cambridge University Press, London (1973).
44. B. Chalmers, *Principles of Solidification,* pp. 150-157, John Wiley & Sons, Inc., New York (1964).
45. W. W. Mullins and R. F. Sekerka, *J. Appl. Phys.,* **35,** 444 (1964).
46. C. A. Knight, *The Freezing of Supercooled Liquids,* p. 87, Van Nostrand, Toronto (1967).
47. H. J. Leamy, C. C. Chang, H. Baumgart, R. A. Lemons, and J. Cheng, *Mater. Lett.,* **1,** 33 (1982).
48. E. Lee, *Mater. Res. Soc. Symp. Proc.,* **35,** 563 (1985).
49. J. C. C. Fan, B-Y. Tsaur, and C. K. Chen, *Proceedings of the Symposium on Energy Beam-Solid Interactions and Transient Thermal Processing,* Vol. 23, pp. 477-489, Materials Research Society (1984).
50. P. W. Mertens, D. J. Wouters, H. E. Maes, A. De Veirman, and J. Van Landuyt, *J. Appl. Phys.,* **63,** 2660 (1988).
51. F. A. Shunk, *Constitution of Binary Alloys,* 2nd Suppl., pp. 157, 572, McGraw-Hill Book Co., New York (1969).
52. R. P. Elliot, *Constitution of Binary Alloys,* 1st Suppl., p. 691, McGraw-Hill Book Co., New York (1965).
53. W. G. Moffatt, *The Handbook of Binary Phase Diagrams,* Vol. II, pp. 3-85, Genium Pub. Co., New York (1987).
54. D. Dutartre, M. Haond, and D. Bensahel, *J. Appl. Phys.,* **59,** 632 (1986).

55. D. Dutartre, in *Proceedings of the Symposium on Silicon-on-Insulator and Buried Metals in Semiconductors,* Vol. 107, pp. 157-168, Materials Research Society (1988).
56. A. B. Limanov and E. I. Givargizov, *Mater. Lett.,* **2,** 93 (1983).
57. L. Pfeiffer, S. Paine, G. H. Gilmer, W. van Saarloos, and K. W. West, *Phys. Rev. Lett.,* **54,** 1944 (1985).
58. D. Dutartre, M. Haond, and D. Bensahel, in *Proceedings of the Symposium on Semiconductor-on-Insulator and Thin Film Transistor Technology,* Vol. 53, pp. 89-94, Materials Research Society (1986).
59. E. Arnoil, U. Landman, S. Ramesh, W. D. Luedtke, R. N. Barnett, C. L. Cleveland, A. Martinez, H. Baumgart, and B. Khan, in *Proceedings of the Symposium on Semiconductor-on-Insulator and Thin Film Transistor Technology,* Vol. 53, pp. 21-27, Materials Research Society (1986).
60. C. P. Grigoropoulos, R. H. Buckholz, and G. A. Domoto, *J. Heat Transfer,* **109,** 841 (1987).
61. J. S. Im, Ph.D. Thesis, Massachusetts Institute of Technology, Cambridge, MA (1989).